WORKSHOP SMART2013
Paris *(France)*, November 25th – 27th, 2014

Simplified wide-column model for the blind prediction shake table test of a U-shaped wall building

Romain Sousa[1], João P. Almeida[2], António A. Correia[3] and Rui Pinho[4]

[1] PhD Student, ROSE Programme, UME School, IUSS Pavia, Pavia, Italy (romain.sousa@umeschool.it)
[2] Postdoctoral Researcher, École Polytechnique Fédérale de Lausanne, Lausanne, Switzerland
[3] Postdoctoral Researcher, National Laboratory for Civil Engineering, Lisbon, Portugal
[4] Assistant Professor, Dept. of Civil Engineering and Architecture, University of Pavia, Pavia, Italy

Introduction

Reinforced concrete (RC) structures with tri-dimensional asymmetries tend to exhibit torsional effects that are of great concern in the field of earthquake engineering, in particular at large ductility levels where they become more relevant [MAN09]. In nuclear facilities, this issue assumes particular relevance considering that these structures are designed to respond essentially in the elastic range with a controlled level of deformations and accelerations when subjected to strong ground motions.

Within the previous framework, the research project SMART 2013 ('Seismic design and best-estimate Methods Assessment for Reinforced concrete buildings subjected to Torsion and non-linear effects') was conducted in order to improve the knowledge on the seismic response of irregular RC structures (experimental test) and to provide reference data for modelling developments and validation (benchmark).

Past blind prediction contests showed that, by making use of appropriate modelling options, the seismic response of structures can be predicted with satisfactory accuracy [SOU14]. Nonetheless, they have also evidenced a significant dispersion of predictions between the different participating teams, as demonstrated by the results obtained in the past blind prediction contest [NEE10].

After a short description of the SMART 2013 mock-up and corresponding loading, the present paper describes the properties of the numerical model used by one the participating teams and the comparison of its results with those obtained from the experiments.

Description of the Test Unit and Loading Protocol

In order to assess the capacity of buildings to withstand earthquake loading and evaluate the level of accelerations that can be transferred to the non-structural components at a given floor, a reduced scale model (1/4 scale) representing, in a simplified way, half part of an electrical nuclear building (Figure 1) was subjected to a large set of dynamic experimental tests. The model was tested at the AZALEE shaking table (Saclay, France) as part of the SMART 2013 project.

This project was supported by the Commissariat à l'Énergie Atomique et aux Énergies Alternatives (CEA) and by Electricité de France (EDF).

Figure 1. SMART 2013 mock-up.

The SMART 2013 mock-up was designed according to the French nuclear regulations and current guidelines for a design spectrum anchored to a peak ground acceleration (PGA) of 0.2 g and a damping ratio of 5% [RIC14].

The experimental mock-up exhibits a trapezoidal shape in plan (Figure 2) and features structural RC walls with openings of variable dimensions, which favour the development of important torsional components. Table 1 summarises the main dimensions of the different walls of the mock-up.

For what concerns the material properties, the concrete compressive strength ranges from 35.5 MPa to 46.6 MPa, whilst the yielding strength of the reinforcement bars varies from 500 MPa to 665 MPa, for the different structural elements.

Assuming that most of the mass is concentrated at the floors, additional mass blocks were fixed to the slabs, totalling about 11 tons per floor in addition to the self-weight of the mock-up (approximately 12 tons). The design drawings can be downloaded from the SMART 2013 website: http://www.smart2013.eu.

Table 1: Dimensions of mock-up structural elements.

Structural component	Length (m)	Thickness (m)	Height (m)
Wall #V01 and #V02	3.1	0.1	3.65
Wall #V03	2.55	0.1	3.65
Wall #V04	1.05	0.1	3.65
Beams	1.45	0.15	0.325
Column	0.2	0.2	3.9

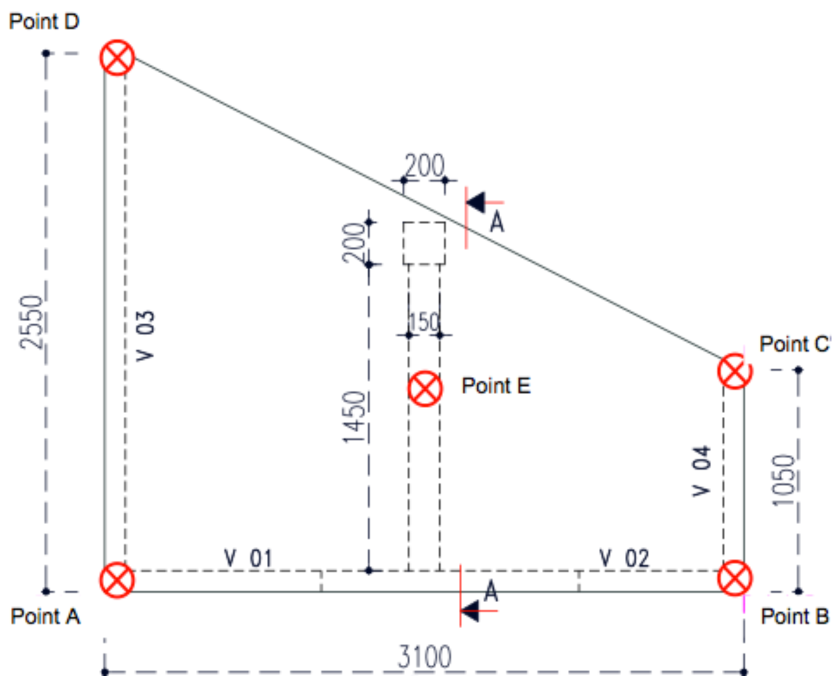

Figure 2. Plan view and dimensions of the mock-up (in mm).

The structure was subjected to a series of seismic excitations that can be subdivided into three groups: synthetic (white noise), natural earthquakes and natural aftershocks. While the first group, featuring very low acceleration amplitudes, aims at identifying the dynamic properties of the system, the second one was defined to impose a progressively larger seismic demand up to the desired design level. Finally the third group considers two ground motions representative of actual aftershock motions. Table 2 shows the input sequence considered for the models discussed below, together with the peak ground acceleration associated to each run.

Table 2: Ground motions' sequence considered in the blind prediction contest.

Run Label	Targeted PGA - X (g)	Targeted PGA - Y (g)	Percentage nominal signal (%)	Realized PGA - X (g)	Realized PGA - Y (g)	Type
6	0.1	0.1	100	0.1	0.1	Synthetic white noise
7	0.1	0.1	50	0.13	0.14	Design signal
9	0.2	0.2	100	0.22	0.23	Design signal
11	0.2	0.11	11	0.21	0.16	Northridge earthquake
13	0.4	0.21	22	0.4	0.21	Northridge earthquake
17	0.8	0.42	44	0.6	0.4	Northridge earthquake
19	1.78	0.99	100	1.1	1	Northridge earthquake
21	0.12	0.07	33	0.14	0.14	Northridge (aftershock)
23	0.37	0.31	100	0.7	0.4	Northridge (aftershock)

In addition, the SMART 2013 international benchmark was composed of four main stages. While the firsts two stages (RUN 6 and 7) were essentially dedicated to perform a dynamic characterization of the mock-up and to calibrate the numerical model based on the linear elastic properties of the mock-up, for the third stage of the benchmark the participants were asked to predict the nonlinear response of the structure when subjected to high intensity seismic motions (RUN 9 to RUN 23, as indicated in Table 2). The accuracy of the predictions is assessed in terms of displacements and accelerations measured at five different points per floor (points A to E in Figure 2) along the three coordinate axes. The fourth stage comprises the evaluation of the structural vulnerability through the determination of vulnerability curves associated with different criteria, considering a database set of 100 horizontal accelerogram pairs. In the present paper, no reference is made to Stage 4 due to lack of time for completing this phase of the contest.

Additional details regarding the experimental protocol and benchmark stages can be found in [RIC14].

Properties of the Numerical Model

Beam-column elements (with concentrated or distributed plasticity) are widely use by structural engineers to simulate the nonlinear response of structures. The application of such formulation has proved to be very suitable for frame structures, combining the accuracy of global response parameters with appreciable computational efficiency, e.g., [BIA2011], [YAZ11] or [BLA12].

Whilst slender frame elements tend to exhibit a response dominated by their flexural component, the response of wall structures combines other deformation mechanisms that are difficult, if not impossible, to be explicitly modelled with beam-column elements implemented in current state-of-the-practice structural analysis programs. In particular, it is difficult to capture the important shear contribution through the development of inclined cracks in the wall panels, the localized response at the wall-foundation interface, or the interaction with adjacent walls, among other effects.

Despite the above mentioned limitations, the model presented in this paper follows a wide-column analogy because it combines the merits of representing a three-dimensional wall structure with inelastic properties while being computationally more efficient, simple and easy to set up when compared to shell or solid finite element models. Furthermore, the authors wanted to verify the applicability limits of frame models for simulating the behaviour of walls wherein shear deformations should be non-negligible. The numerical model considered was built in the SeismoStruct platform ([SEI13]), using a number of modelling assumptions that are briefly described hereafter.

The sectional properties of the walls were defined considering the (confined) concrete uniaxial nonlinear model proposed by [MAN88] and the well-known steel stress-strain relationship proposed by [MEN73]. These models are numerically stable and able to capture the behaviour of complex cyclic loading histories.

Given that in a wide-column analogy the vertical elements (walls) are reproduced with line elements, it is not possible to connect directly adjacent elements or define a continuous slab to simulate the floors. Hence, special care should be taken with the definition of the connection between the elements. The connection between adjacent walls was guaranteed through the definition of rigid elastic elements that link the centre of the wall (where the frame elements is placed) to the corner where the adjacent wall is connected. It is important to note that the torsional stiffness of these elements should be very low in order to avoid the (unrealistic) transfer of the corresponding sectional forces to the adjoining wall. Moreover, considering the restraining effect of the slab, it was assumed that the relative deformation between the walls, in particular in the out-of-plan direction, was negligible. For that purpose, regarding the modelling of the slabs, a grid of elastic elements approximately reproducing the estimated elastic stiffness of the RC slab was defined, connecting the main structural nodes. Despite requiring a larger number of elements, this solution proved to be numerically more stable, for this particular structure, than the simpler alternative of defining a rigid diaphragm.

In view of the absence of a continuous slab in the numerical model, the additional mass blocks distributed along the slab of the mock-up were lumped at the main structural nodes according to the associated tributary areas. The self-weight of the mock up was implicitly modelled through the specific weight of the materials.

An important decision when modelling a frame structure for seismic analysis is related to the choice of the element model. Lumped plasticity approaches are simpler and computationally lighter, but they do not capture the spread of inelasticity throughout the member as the alternative distributed plasticity models do. Within the later group, force-based (FB) and displacement-based (DB) formulations are usually available, which verify equilibrium along the element length in an exact and average way, respectively. Despite this clear advantage of the FB approach, the analyses performed with FB elements exhibited important convergence difficulties when subjected to large ductility demands. For this reason, the model adopted considers four DB elements for each RC wall.

As previously mentioned, the majority of beam-column formulations available in current software packages do not account for shear deformations. Hence, in order to consider such additional flexibility of the wall elements, zero-length shear springs were introduced at mid-height of each wall. The stiffnesses of these springs were determined according to the recommendations proposed by [BEY08]:

$$k_S = \frac{GA_S}{h_{sp}} \qquad (1)$$

where G is the shear modulus, h_{sp} is the vertical spacing between shear springs and A_s is the shear area, which was taken as $0.8A_{gross}$. The stiffness computed for each wall was then assigned to the corresponding spring in the in-plane direction, while all other degrees of freedom were rigidly connected (the contribution of shear flexibility in the out-of-plan direction being neglected).

Although the modelling choices of this wide-column model had the purpose of providing an improved response at larger ductility levels, it is also important to evaluate its dynamic properties at initial elastic conditions. Hence, a complementary model with elastic shell elements was built in SAP2000 [CSI09], additionally incorporating the contribution of the mass and flexibility properties of the shake table subsystem (Figure 3, left).

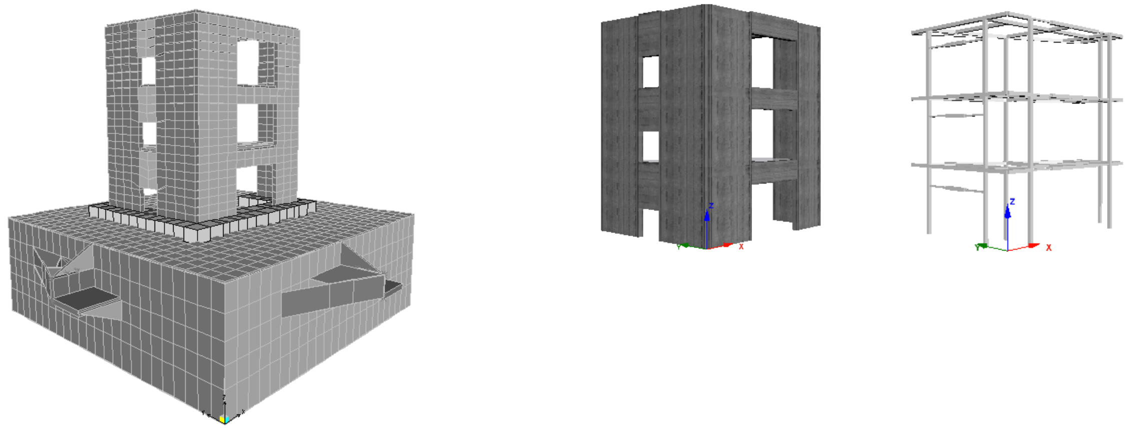

Figure 3. Numerical model with shell elements (left) and wide-column analogy (centre and right).

Given that the experimental measurements provided are associated with the complete system, i.e., RC structure and shake table, a first comparison was made with respect to the complete numerical model constructed with shell elements. Once this model has been calibrated, in terms of matching its modal frequencies to the experimental ones, a new shell model was considered without the contribution of the shake table subsystem, i.e., assuming that all nodes at the base of the structure were fixed. This third model was defined in order to allow the direct comparisons of the model with shell elements with the one assuming the wide-column analogy with a fixed base (Figure 3, right). Since the seismic input used in the numerical model was the one measured on top of the shake table, and ignoring the local deformations of the shake table, the dynamic interaction effects between the mock-up and the shake table subsystem are directly accounted for in the input motion. The authors are aware that this claim is correct only while the mock-up responds in the elastic range and if the numerical model exactly reproduces its elastic dynamic characteristics. Otherwise, a complete simulation should be performed that includes such dynamic interaction. Time constraints and lack of information prevented the authors from attempting to pursue such ambitious task.

The dynamic properties obtained with the shell model including the shake table reveal a slight difference with respect to the experimental values for the three first periods of vibration (Table 3 – 2nd and 3rd columns). Similar differences were again observed between the shell elements model without the shake table and the one using the wide-column approach (Table 3 – 4th and 5th columns). Considering the potential variability associated with the measurements, material properties, geometry, mock-up transportation, etc., it was considered that the differences in the computed values were within a reasonable tolerance.

Table 3: Comparison between the periods of vibration measured in the experimental test and computed with different numerical models.

	Period (s)			
	Mock-up + Table		Mock-up	
	Measured	SAP2000	SAP2000	SeismoStruct
Mode 1 (x-dir.)	0.159	0.184	0.111	0.109
Mode 2 (y-dir.)	0.127	0.120	0.061	0.068
Mode 3 (torsion)	0.060	0.053	0.034	0.040

For what respects the nonlinear dynamic analyses (which, as noted above, were run using the equivalent wide-column frame elements), it is relevant to mention that the Hilber-Hughes-Taylor integration scheme [HIL77] was deliberately adopted, as its numerical damping filters out the contribution of higher modes, thus avoiding potential spurious response. The time step of the analysis was kept constant with respect to the input ground motions provided by the organizing commission, i.e., about 0.001 s.

In addition to the energy dissipated through material hysteresis, an additional source of energy dissipation was defined through equivalent viscous damping (EVD) defined with a Rayleigh damping model with 2.5 % of critical damping assigned to the first and second fundamental modes of vibration. This relatively large damping value, in comparison to what was observed in other validation analyses [SOU14], intends to account for hysteretic shear response, not accounted for in the wide-column modelling adopted herein.

During the experimental campaign, the specimen was subjected to several consecutive ground motion of varying intensity as indicated in Table 2. Figure 4 illustrates the set of records considered for the numerical model. The analyses comprise RUN 9 to RUN 23 in order to account for the cumulative damage induced to the structure by each individual earthquake. The first two records (RUN 6 and RUN 7) where not considered given their low amplitude. A 10 s gap between each record was defined in order to allow the structure to return to rest after each seismic excitation.

Results

The present section shows a summary of the results obtained in terms of relative displacements measured with respect to the shake table and absolute accelerations of point B and D (see Figure 2) at the third storey of the mock-up.

While the identification of maximum values measured during strong ground motions is of primary importance, the response during lower intensity and aftershocks allows for an assessment regarding the response under essentially elastic behaviour as well as the damage accumulation along the large set of ground motions. The time-histories of accelerations and displacements illustrated in Figure 5 and Figure 6 show the comparison between the experimental and numerical response of the structure during the strongest motion of the set, RUN 19. The title of each plot indicates (separated by a dash) the Run, point, storey and directions, respectively. It is important to note that the initial value of each plot was set to zero in order to avoid possible incongruences in the residual deformation resulting from intermediate experimental tests.

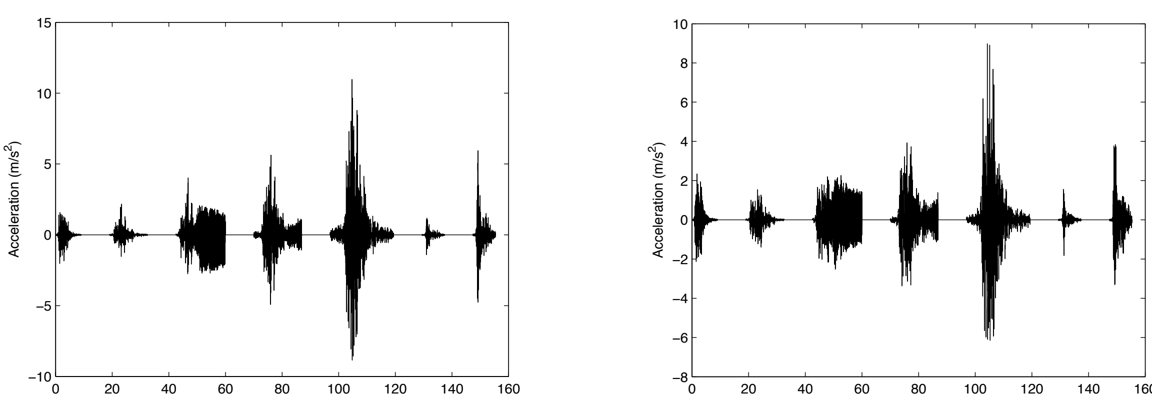

Figure 4. Ground motion considered in the numerical analyses: X (left) and Y (right) direction.

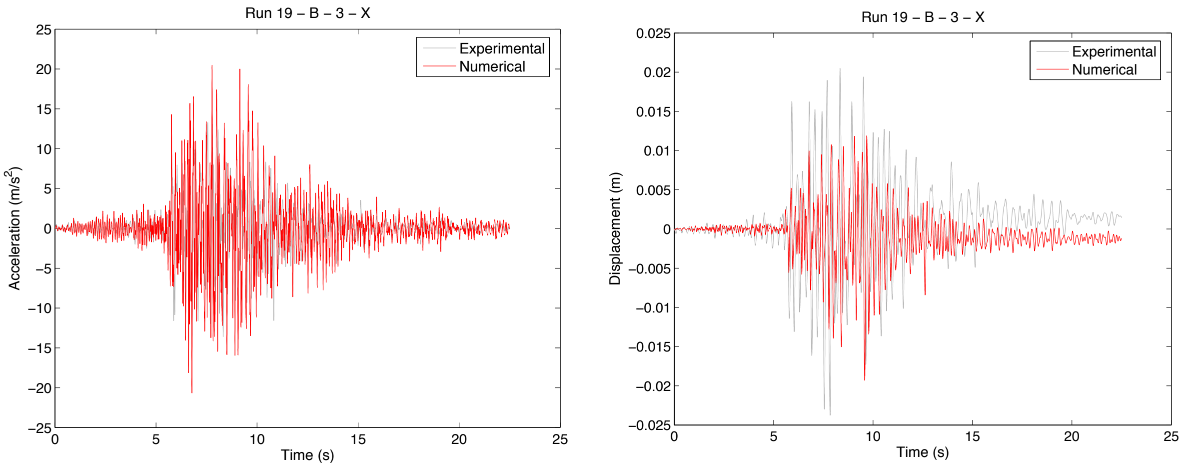

Figure 5. History of accelerations and displacements – RUN 19, X-direction, point B.

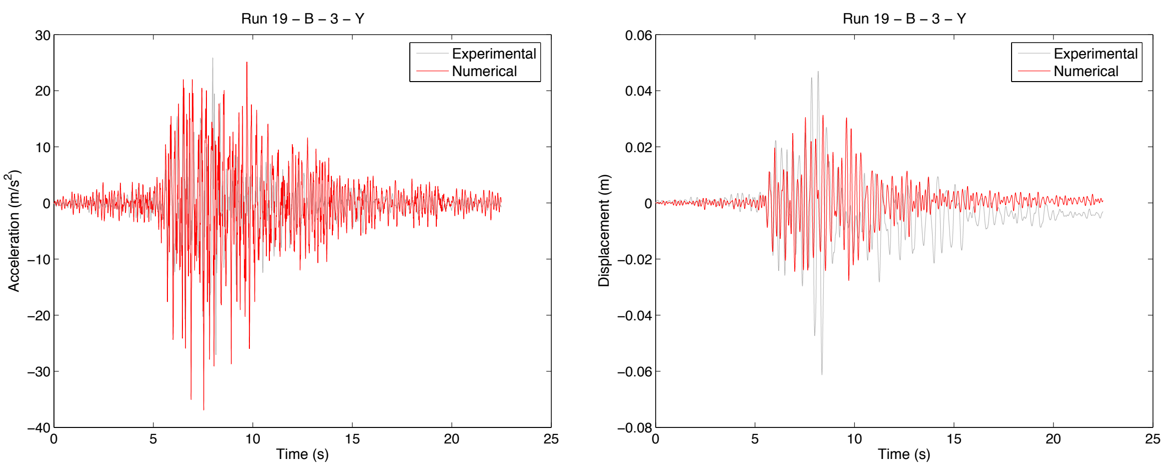

Figure 6. History of accelerations and displacements – RUN 19, Y-direction, point B.

The results presented above show that the numerical accelerations seem to be relatively well predicted, while displacements measured during RUN 19 tend to be underestimated by the numerical model. An important contribution to the differences observed could be attributed to the rupture of the connection between the RC walls and the foundation observed during the experimental test, which seems to be associated with the slippage of the longitudinal reinforcement linking these two elements. Moreover, it is important to note that the numerical model does not take into account the additional flexibility resulting from strain penetration effects.

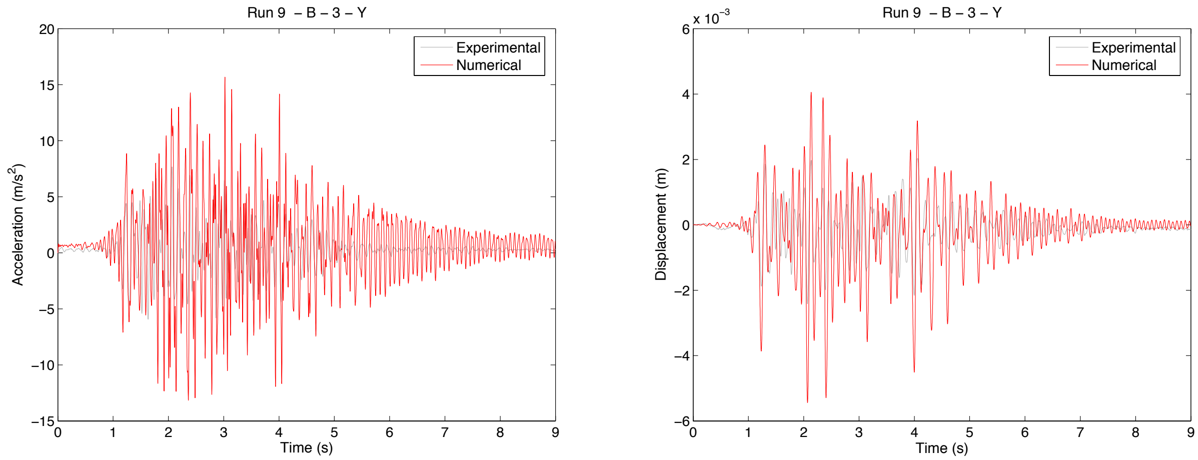

Figure 7. History of accelerations and displacements – RUN 9, Y-direction, point B.

The results presented in Figure 7 show that under lower seismic input (RUN 9), the differences are also relevant, but now the accelerations and displacements are overestimated. At this stage, the structure is undamaged and the response is essentially governed by its modal properties. This difficulty in reproducing the (essentially) elastic behaviour can be attributed to possible incongruences associated with the material properties, namely tension stiffening effects, variability in the tensile strength and modulus of elasticity of the concrete. Moreover, it is important to recognize potential limitations associated with the wide-column model regarding the definition of the slab, connections between adjacent walls and the contribution of shear deformations.

The results presented in Figure 8 illustrate the comparison of accelerations and displacements during the last ground motion (RUN 23). Similarly to what was observed during RUN 19, the numerical displacements are underestimated with respect to the experimental ones. Moreover, as it is possible to observe in the same figure, the modelled structure oscillates with a higher frequency than the model tested in the shake table. Hence, and considering the lower displacement demand induced in the previous runs (and consequently lower structural damage), the structure presents a larger stiffness, which results in potentially lower structural deformations.

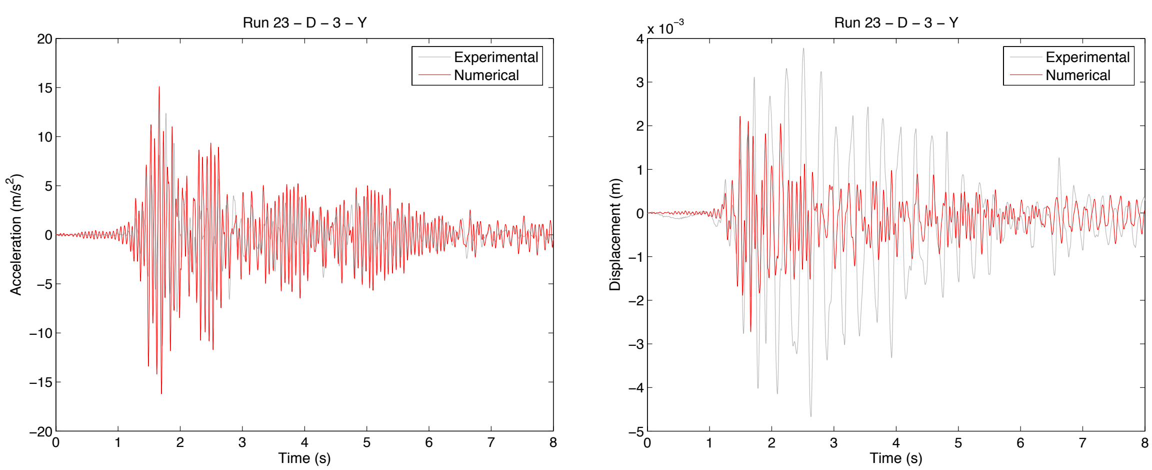

Figure 8. History of accelerations and displacements – RUN 23, Y-direction, point D.

Finally, Table 4 shows the relative error associated with the maximum accelerations and displacements obtained during RUN 9, 19 and 23, determined with the following expression:

$$Error_{Max.} = \frac{max\left(EDP_{computed}\right) - max\left(EDP_{measured}\right)}{max\left(EDP_{measured}\right)} \qquad (2)$$

where *EDP* represents the structural accelerations or displacements.

Table 4: Relative error associated with the accelerations and displacements measured along X and Y directions during RUN 19.

		Acceleration		Displacement	
		X	Y	X	Y
RUN 9	Point B	1.73	1.05	0.83	1.25
	Point D	1.02	2.14	0.16	0.60
RUN 19	Point B	0.42	0.36	-0.19	-0.49
	Point D	0.23	0.05	-0.43	-0.33
RUN 23	Point B	0.27	0.54	-0.40	-0.49
	Point D	0.00	0.31	-0.05	-0.42

Based on the results presented in the previous table, it is clear that the accuracy of the response evaluated at point B and D varies along the different runs and directions. These observations suggest that, the dynamic properties of the numerical model (namely its torsional component), may present some deviations with respect to the structure tested on the shake table.

Conclusions

An experimental campaign sponsored by CEA and EDF was conducted to investigate the seismic response of asymmetric wall structures subjected to strong ground motions. At the same time, a benchmark contest was launched to evaluate the capabilities of current numerical tools, as well as to identify modelling strategies that result in more accurate estimation of structural response parameters. After a brief description of the experimental campaign, the present paper focuses on the description of the modelling decisions and strategy adopted by one of the benchmark participating teams.

The displacements and accelerations computed by the model under low seismic intensity present non-negligible deviations when compared with the experimental results. These deviations may be associated to an eventual dispersion of material properties and to the simplifications associated with the use of a wide-column model, namely regarding the definition of the slab, connections between adjacent walls and the contribution of shear deformations.

Furthermore, it was verified that under strong seismic motions, the structural displacements were consistently underestimated. It is believed that the additional flexibility (base rotation) resulting from the separation between the RC wall and the foundation during the experimental test contributed greatly to the difference observed. In addition, it is important to note that important numerical convergence difficulties precluded the consideration of alternative modelling solutions that, in the authors' opinion, would render more accurate response parameters. It is recalled that the numerical model does not account for strain penetration effects, while the shear mechanism associated with the response of structural RC walls was modelled with linear shear springs, which represents an extremely simplified approach. Moreover, the use of FB elements, possibly including the nonlinear shear behaviour [COR14], together with better estimates of the material properties, tension stiffening effects, etc., could also contribute to improve the numerical simulation of the experimental test.

Overall, and despite the obvious limitations implicit to the use of beam-column elements to simulate the response of RC walls, it is believed that the application of wide-column models could be a reliable and efficient option to simulate the seismic response of wall structures, provided that the structural complexity of the model, and hence the potential to present numerical convergence difficulties, does not prevent the consideration of the most appropriate numerical modelling options.

References

[NEE10] NEES@UCSD (2010). "Concrete Column Blind Prediction Contest," Available from: http://nisee2.berkeley.edu/peer/prediction_contest

[BEY08] Beyer, K., A. Dazio, and N. Priestley (2008). "Inelastic Wide-Column Models for U-Shaped Reinforced Concrete Walls," *Journal of Earthquake Engineering*, 12(sup1), 1–33.

[BIA11] Bianchi, F., R. Sousa, and R. Pinho (2011). "Blind Prediction of a Full-Scale RC Bridge Column Tested Under Dynamic Conditions" *Proc., COMPDYN*, Curfu, Greece.

[BLA12] Blandon, C. (2012). "Sensibility of Non Linear Time History Analysis of a RC Column Using Large Scale Shaking Table Results as Benchmark" *Proc., WCEE*, Lisbon, Portugal.

[CSI00] CSI (2009), "SAP2000 v.14" Linear and nonlinear static and dynamic analysis and design of three-dimensional structures, Computer and Structures, Inc.

[HIL77] Hilber, H., T. Hughes, and R. Taylor (1977). "Improved Numerical Dissipation for Time Integration Algorithms in Structural Dynamics," *Earthquake Engineering and Structural Dynamics*, Vol. 5, 283–292.

[MAN88] Mander, J., N. Priestley, and R. Park (1988). "Theoretical Stress-Strain Model for Confined Concrete," *J. Structural Engineering*, 114(8), 1804–1826.

[MAN09] Mansuri, M. (2009). "Torsional Efects on the Inelstic Seismic Response of Structures," PhD thesis, University of California, California, USA.

[MEN73] Menegotto, M., and P. Pinto (1973). "Method of Analysis for Cyclically Loaded R.C. Plane Frames Including Changes in Geometry and Non-Elastic Behavior of Elements under Combined Normal Force and Bending" *Proc., Symp. Resistance and Ultimate Deformability of Structures Acted on by Well-Defined Repeated Loads*, Lisbon, Portugal.

[RIC14] Richard, B., and T. Chaudat (2014). "Presentation of the SMART 2013 International Benchmark", CEA-EDF.

[SEI13] Seismosoft (2013), "SeismoStruct v.6.5 - A Computer Program for Static and Dynamic Nonlinear Analysis of Framed Structures", Available from URL: www.seismosoft.com.

[SOU14] Sousa, R., A. Correia, J. Almeida, and R. Pinho (2014). "Blind Prediction Tests as a Benchmark to Improve the Seismic Response of Fibre Models" *Proc., of the 2nd European Conference on Earthquake Engineering and Seismology*, Istanbul, Turkey.

[YAZ11] Yazgan, U., and A. Dazio (2011). "Simulating Maximum and Residual Displacements of RC Structures: I. Accuracy", *Earthquake Spectra*, 27(4), 1187–1202.

[COR14] Correia, A.A., J.P. Almeida and R. Pinho (2014). "Force-based higher-order beam element with flexural-shear-torsional interaction in 3D frames. Part I: Theory," *Engineering Structures*, Accepted for publication.